NANO LETTERS

Letter

pubs.acs.org/NanoLett

Stretchable Photonic Crystal Cavity with Wide Frequency Tunability

Chun L. Yu,[†,%,∥] Hyunwoo Kim,[†,%] Nathalie de Leon,[†,‡] Ian W. Frank,[§] Jacob T. Robinson,[†,#] Murray McCutcheon,[§,&] Mingzhao Liu,[†,⊥] Mikhail D. Lukin,[‡] Marko Loncar,[§] and Hongkun Park*[,†,‡]

[†]Department of Chemistry and Chemical Biology, [‡]Department of Physics, and [§]School of Engineering and Applied Sciences, Harvard University, Cambridge, Massachusetts 02138, United States

Supporting Information

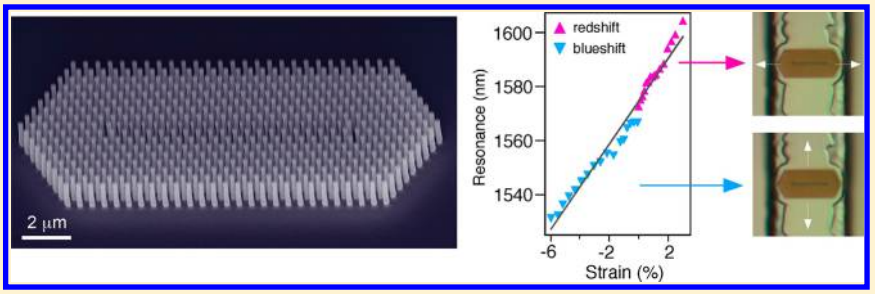

ABSTRACT: We report a new approach for realizing a flexible photonic crystal (PC) cavity that enables wide-range tuning of its resonance frequency. Our PC cavity consists of a regular array of silicon nanowires embedded in a polydimethylsiloxane (PDMS) matrix and exhibits a cavity resonance in the telecommunication band that can be reversibly tuned over 60 nm via mechanical stretching—a record for two-dimensional (2D) PC structures. These mechanically reconfigurable devices could find potential applications in integrated photonics, sensing in biological systems, and smart materials.

KEYWORDS: *Photonic crystal, nanowire, resonance frequency tuning, flexible device*

Photonic crystals (PCs), which enable tight confinement and precise control of optical fields in the micrometer-scale dimensions, provide a promising platform for on-chip photonic and optoelectronic devices, such as lasers, filters, sensors, and quantum optical devices.[1−5] These structures typically consist of arrays of holes etched into a semiconductor substrate that lacks mechanical flexibility. Consequently, the control over their optical properties over a wide frequency range is difficult without making permanent changes to the device geometry or materials.[6,7]

To date, many different approaches have been developed to tune the resonance frequency of PC cavities postfabrication. Methods based on temperature change,[8] free carrier injection,[9] and gas condensation[10] enable reversible frequency tuning but suffer from limited tuning ranges (typically less than 10 nm) because of small changes in the refractive index contrast afforded by these methods. In contrast, compositional or structural changes to the PC cavities allows wider tuning ranges, but the resulting changes are irreversible,[6,7] limiting their utility. Clearly, reversible tuning of cavity resonances over a wide range remains a significant challenge.

In this Letter, we report a new strategy to address this problem by embedding a nanowire (NW)-based PC in a low-index polydimethylsiloxane (PDMS) substrate (Figure 1), forming a mechanically compliant composite structure. As demonstrated in a variety of other photonic structures, mechanical deformation is an effective way to yield large resonance tuning.[11−14] The cavity within our PC is defined by reducing the diameter of 19 NWs arranged in a line within a 2D hexagonal NW array. The length of our resonant cavity can be reversibly stretched or compressed, providing a facile route to tune the resonance frequency over a wide range.

Because the dielectric contrast of our PC is essentially the inverse of that found in a traditional PC cavity defined on a high-index semiconductor substrate, our PC cavity supports transverse magnetic (TM) modes (the electric field of the cavity mode is polarized along the NW length and perpendicular to the PC plane).[2,15,16] We used both finite-element (MIT photonic bands) and finite-difference time-domain (FDTD, Lumerical) simulations to design and optimize the NW dimensions and spacing (see Supporting Information). As shown in Table S1, the NW-polymer PC cavity can support several well-defined resonant modes with theoretical quality (Q) factors exceeding 4000.

Figure 1a lays out the fabrication scheme for flexible PCs. We fabricated the PC cavities by first defining an array of NWs via a top-down silicon etching process[17] (Figure 1b). We then transferred them into the PDMS matrix after thinning the NW bases through a reactive ion etching process (Figure 1c; see Supporting Information for detailed fabrication processes). Figures 1d,e show the completed PC cavity in a PDMS mesa that elevates the cavity from the bulk PDMS substrate.

We probed the optical properties of the PC cavities by exciting their photonic modes using the evanescent field of a

Received: October 29, 2012
Revised: December 11, 2012
Published: December 17, 2012

   dx.doi.org/10.1021/nl303987y | *Nano Lett.* 2013, 13, 248−252

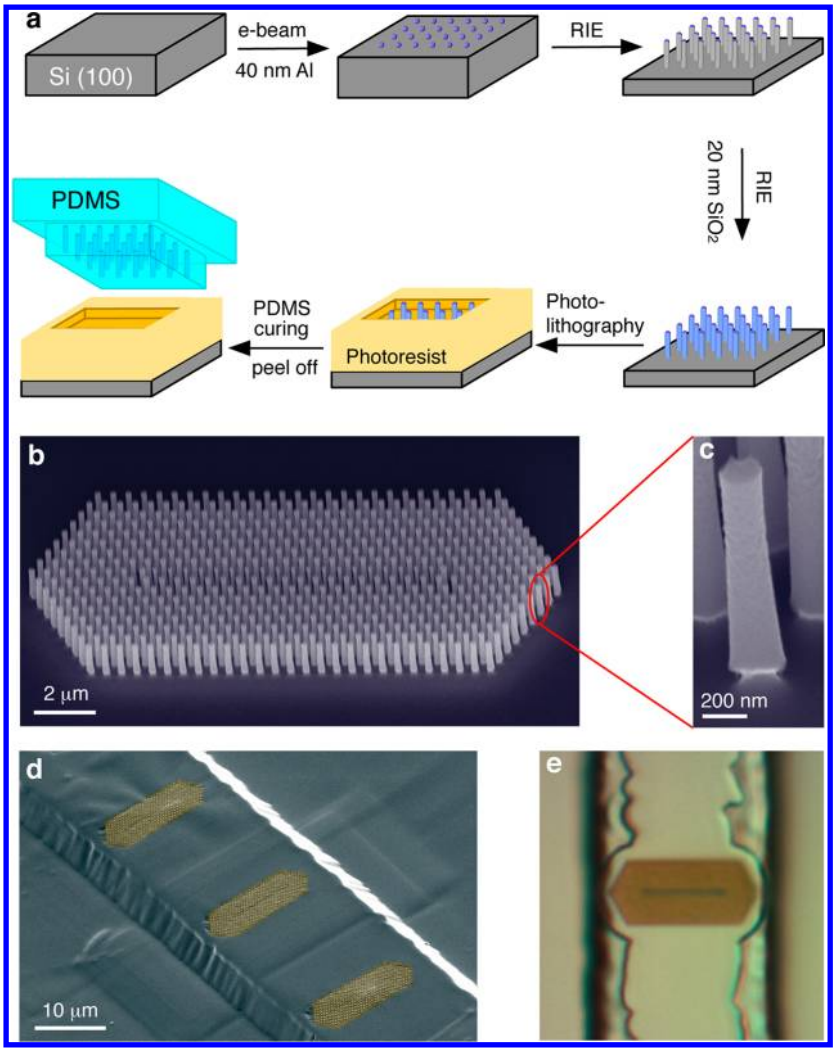

Figure 1. Flexible PC cavities. (a) Schematic for flexible PC cavity fabrication: we define the PC patterns on Si (100) wafer by electron-beam lithography; deposit 40 nm Al as an etch mask; etch silicon to form Si NWs; deposit 20 nm SiO_2 by atomic layer deposition; selectively etch SiO_2 on the substrate; thin the NW bases by etching; pattern a window by photolithography; pour and cure PDMS; and then finally peel off the PDMS. (b) Scanning electron microscope (SEM) image of the PC cavity tilted at 45°. Design dimensions: regular NW diameter is 200 nm; defect NW diameter is 140 nm; NW length is 1.2 μm. The hexagonal lattice spacing is 500 nm. (c) Zoom-in view of an undercut NW at the PC edge, also tilted at 45°. (d) SEM image of the PDMS mesa structure containing several PC cavities. (e) Optical image of the top-down view of a PC embedded in PDMS. The dark line in the middle of the PC is the line defect.

tapered fiber (Figure 2a, see Supporting Information).[18,19] When the laser polarization was perpendicular to the device plane, the transmission spectrum of a PC cavity showed two peaks that were clearly above the background Fabry-Pérot interference fringes (Figure 2b). These two peaks disappeared when the laser polarization was changed to be parallel to the device plane, confirming that the peaks indeed correspond to TM modes of the cavity. By fitting the observed peaks to Lorentzian functions, we determined the line width of each mode. The Q factors of the two modes were determined by dividing the peak wavelength by the line width, yielding Q factors of ~3300 and 3000, respectively.

We assigned these two peaks as e1 and e2 modes (Figure 2c), the two highest-Q modes obtained from FDTD simulations (Q_{theory} ~ 25 000 and 5000). This assignment was based on several factors. First, these two modes are most prevalent in line-defect photonic crystal cavities similar to our PC design.[20,21] Second, although the absolute values of the resonance positions differ from those predicted from FDTD simulations (most likely due to fabrication imperfections such as tapering of the NW sidewalls), the experimental peak spacing of 2.4 nm is close to the 2 nm spacing between the calculated e1 and e2 resonant wavelengths. Finally, and most importantly, the relative intensities of the e1 and e2 modes changed when we altered the fiber alignment, in a manner expected from their mode profile. The e2 mode has a node at the cavity center, and consequently, the excitation of this mode was suppressed when the excitation fiber was positioned across the cavity center at an angle with respect to the cavity line, as shown in Figure 2d. When we moved the fiber away from the cavity center, however, stronger excitation of the e2 mode occurred as expected from better mode overlap. We note that the positions of the resonances in Figure 2d are blue-shifted by 6 nm compared to those in Figure 2b because the dielectric pertubative effects of the fiber are reduced as the fiber is skewed by 5°.[19]

Because our PC cavities are defined on a mechanically compliant substrate, the resonance wavelengths of the cavities

dx.doi.org/10.1021/nl303987y | Nano Lett. 2013, 13, 248−252

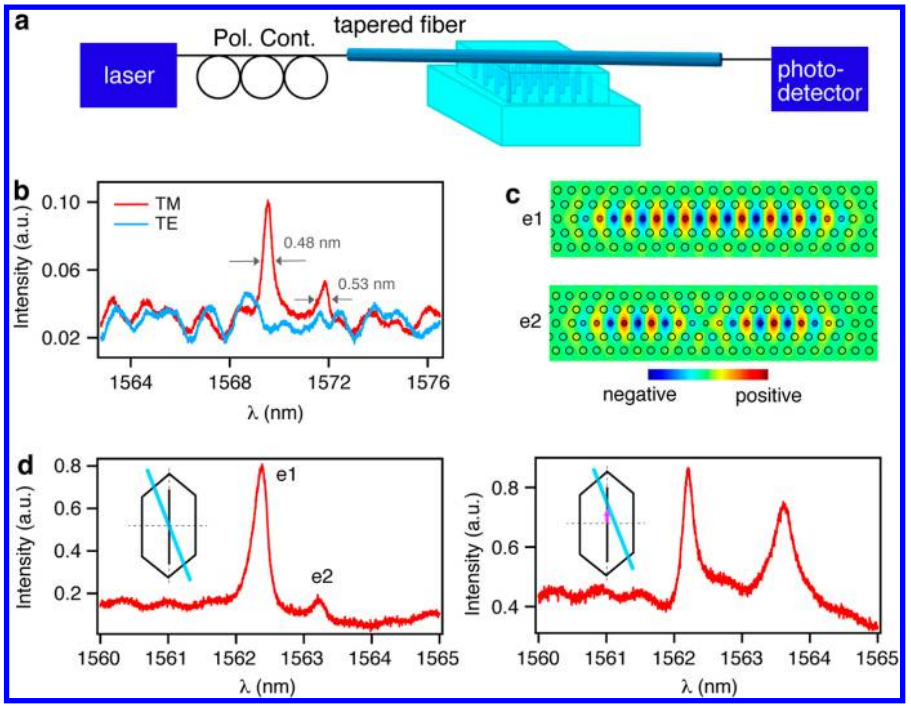

Figure 2. Transmission measurements for mode identification. (a) Schematic for transmission measurements. Tapered SMF-28 fiber, coupled to a laser, a polarization controller (Pol. Cont.) and a photodetector, is lowered down to be in contact with the PC cavity. (b) Transmission spectra of TE and TM polarizations. Lorentzian fit gives FWHM of 0.48 and 0.53 nm for both peaks, respectively. (c) Electric-field amplitudes for e1 and e2 modes. (d) When the tapered fiber was aligned off-axis from the line defect, the e2 mode was suppressed (left panel). The intensity of the e2 mode increased (right panel) when the fiber was moved off-centered from the defect. The insets show the cartoon drawings of fiber on the cavity. The angle between the fiber (blue line) and the line defect (vertical black line) is exaggerated for visual convenience. The crossing point of the dashed lines indicates the cavity center.

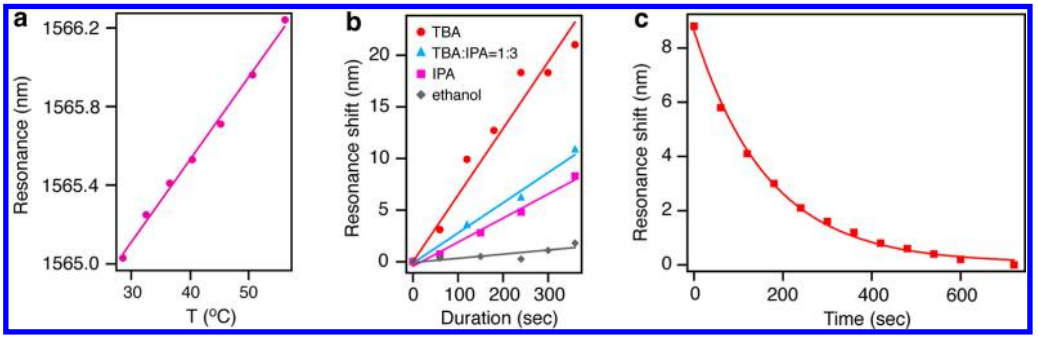

Figure 3. Resonance shift as a function of temperature and solvent swelling. (a) Resonance peak (e1) red-shifted as temperature increased. (b) Resonance (e1) shift as a function of time that PDMS stayed in a solvent bath. (c) As TBA evaporated over time, the resonance moved back to the original position (without solvent swelling) with exponential time dependence.

can be tuned in a variety of ways. First, similar to conventional PC cavities,[8] our cavity can be tuned thermally using a Peltier stage to heat the PDMS. To track the tuning of the resonance wavelength, we monitored the e1 mode because it was the more prominent of the two peaks. As expected from the thermo-optic effect from Si and thermal expansion from PDMS, we observed a linear red-shift of 0.04 nm/°C when we raised the temperature of the PC cavity (Figure 3a).

In addition to temperature change, swelling of the PDMS matrix by exposure to chemical solvents can also tune the resonance frequencies. Specifically, we investigated the optical response of our cavities to three common organic solvents: ethanol, isopropanol (IPA), and *tert*-butanol (TBA), whose maximum swelling ratios in PDMS at room temperature are 4%, 9%, and 21%, respectively.[22] Figure 3b plots the resonance shift as a function of time spent in the solvent (the transmission spectrum was recorded 150 s after the sample was removed from the solvent). Within the experimental time window (360 s), all four solvents caused a linear red-shift of cavity resonances. Furthermore, solvents with larger swelling ratios induced larger resonance shifts for a given immersion period. Because the refractive indices for ethanol, IPA, and TBA are all smaller than that of PDMS, the refractive index of the swollen PDMS should be smaller compared to regular PDMS,[23] leading to a blue-shift of the cavity resonance if the index change were the main cause of the observed shift. Experimentally, we observed red-shifts of the resonances instead (Figure 3b), indicating that the dominant factor for the observed resonance shift was cavity length increase due to PDMS swelling. Indeed, we measured the PDMS expansion to be ~2% at the maximum resonance shift induced by TBA, coinciding with the measured 1.4% shift in the resonance wavelength. As TBA evaporated, the

dx.doi.org/10.1021/nl303987y | *Nano Lett.* 2013, 13, 248−252

wavelength of the resonance returned to the preswelling value with a typical time constant of 165 s (Figure 3c), confirming that reversible tuning is indeed possible.

Finally, we measured the optical response of our cavity under uniaxial mechanical stretching. Stretching the cavity allows us to alter the cavity length and thereby shift the resonance wavelength. To lengthen the cavity, we stretched it along the cavity line using a custom-built mechanical stage. To compress the cavity, we stretched it orthogonally to the cavity line. Because the Poisson ratio of PDMS is close to 0.5, when it is stretched orthogonal to the cavity line, it shrinks in the directions orthogonal to the strain in order to conserve its volume—thereby compressing the cavity length.[24] As expected, the stretching along the cavity line resulted in a red-shift of the resonance up to 32 nm before the amplitude of the e1 mode fell below the background level (Figure 4a,b). The stretching in the orthogonal direction, on the other hand, caused a resonance blue-shift by up to 35 nm (Figure 4b), yielding the total resonance tuning of 67 nm via mechanical deformation. As the lattice periodicity is perturbed, the Q factor changes as shown in Figure 4a inset and Figure S2. Ultimately, Q factor degradation at larger strains limits the range of resonance frequency tuning. The resonance shifted linearly as a function of strain for both directions, demonstrating that the PDMS matrix was within the linear elasticity regime.[12,25] Importantly, when strain was removed, the cavity resonance returned to the original value, confirming that the method allows for both reversible and wide-bandwidth tuning.

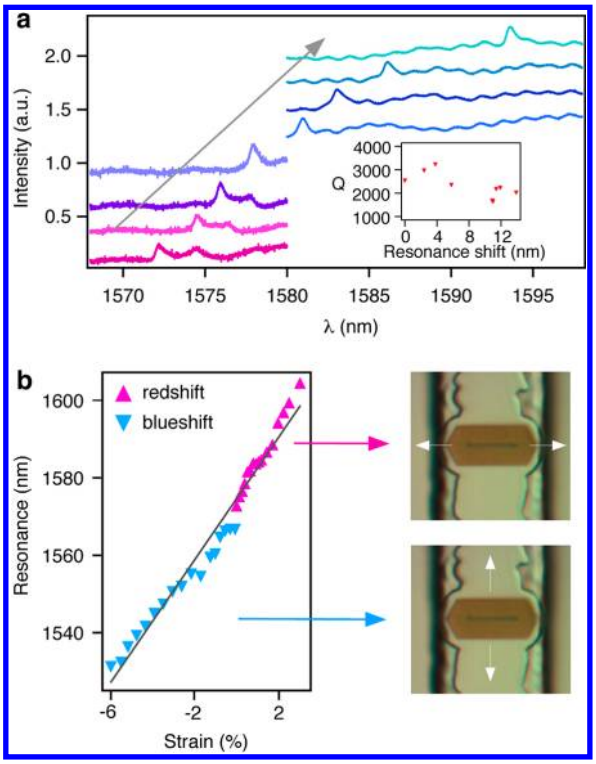

Figure 4. Cavity resonance shift under mechanical stretching. (a) Representative transmission spectra showing resonance shift as the PDMS was being stretched. The discontinuity comes from the fact that when the resonance shifts out of the scanning range of the first laser (1480−1580 nm), a second laser (1580−1680 nm) was used for measurement. Inset: Q factor (e1 mode) as a function of resonance shift. (b) Resonance (e1) shift as a function of strain along the cavity. The black line is a linear fit. Strain is defined as the percentage change of the cavity length. Two stretching directions were explored (as shown in the optical images): along or orthogonal to the line defect.

Although changes to the cavity length likely dominate the observed resonance shift, the anisotropic stretching of the PDMS also alters the lattice constant. To determine if these two factors could accurately describe our observations, we simulated the resonance shift using FDTD after adjusting the cavity dimensions to those corresponding to the maximum strain situation, assuming uniform strain across the entire structure (the simulations of mechanical deformation by COMSOL confirm the validity of this assumption (see Supporting Information)). The simulation results confirmed a red-shift of 30 nm for strain along the line defect and a blue-shift of 29 nm for strain orthogonal to the defect, in very good agreement with experimental observation.

The results presented here demonstrate that a combination of high-index dielectrics and stretchable polymeric materials can be used to construct flexible PC cavities with broadband, controllable, and reversible frequency tuning. This resonance shift, in turn, can be utilized to quantitatively sense the strain exerted on the cavity. Moreover, similar strategies could be employed in other material systems for operation at other wavelength ranges, in active materials to enhance light−matter interactions, and to realize new flexible photonic devices with increasingly complex functionalities including waveguides,[26] modulators,[27] and metamaterials.[28] For instance, it should be possible to construct flexible photonic crystal cavities using diamond nanowire arrays,[29] where the cavity resonance can be tuned to the zero-phonon line of nitrogen-vacancy centers for quantum electrodynamics (QED) experiments.[30]

■ ASSOCIATED CONTENT

Supporting Information

FDTD simulations, materials and methods, calculation of strain on PC cavity, Q analysis, mechanical deformation simulations. This material is available free of charge via the Internet at http://pubs.acs.org.

■ AUTHOR INFORMATION

Corresponding Author

*E-mail hongkun_park@harvard.edu.

Present Addresses

[‖]The David H. Koch Institute for Integrative Cancer Research, Massachusetts Institute of Technology, Cambridge, MA 02139.
[⊥]Center for Functional Nanomaterials, Brookhaven National Laboratory, Upton, NY 11973.
[#]Departments of Electrical and Computer Engineering & Bioengineering, Rice University, Houston, TX 77005.
[&]Lux Research Inc., Boston, MA 02110.

Author Contributions

The manuscript was written through contributions of all authors. All authors have given approval to the final version of the manuscript.

Author Contributions

[%]These authors contributed equally.

Notes

The authors declare no competing financial interest.

■ ACKNOWLEDGMENTS

The authors gratefully acknowledge the support from NSF (PHY-0969816), NSF CUA (PHY-1125846), ONR (FA95550-12-1-0024), AFOSR (FA2386-10-1-4064-DOD 35CAP), and

Packard Foundation, and the use of facilities at the Center of Nanoscale Systems at Harvard University. N.d.L. acknowledges Element Six for postdoctoral fellowship funding. The authors thank Dr. Kwanyong Seo, Dr. Qimin Quan, Prof. Dirk Englund, Alan Dibos, and Marsela Jorgolli for helpful discussions.

■ ABBREVIATIONS

PC, photonic crystal; 2D, two-dimensional; NW, nanowire; PDMS, polydimethylsiloxane; TM, transverse magnetic; *Q*, quality; FDTD, finite-difference time-domain; QED, quantum electrodynamics.

■ REFERENCES

(1) Vahala, K. J. *Nature* **2003**, *424*, 839−846.
(2) Joannopoulos, J. D.; Johnson, S. G.; Winn, J. N.; Meade, R. D. *Photonic Crystals: Molding the Flow of Light*, 2nd ed.; Princeton University Press: New York, 2008.
(3) Mabuchi, H.; Armen, M.; Lev, B.; Loncar, M.; Vuckovic, J.; Kimble, H. J.; Preskill, J.; Roukes, M.; Scherer, A. *Quantum Inf. Comput.* **2001**, *1* (special issue on Implementationof Quantum Computation), 7−12.
(4) Ellis, B.; Mayer, M. A.; Shambat, G.; Sarmiento, T.; Harris, J.; Haller, E. E.; Vuckovic, J. *Nat. Photonics* **2011**, *5*, 297−300.
(5) Loncar, M.; Scherer, A.; Qiu, Y. *Appl. Phys. Lett.* **2003**, *82*, 4648−4650.
(6) Yang, X.; Chen, C. J.; Husko, C. A.; Wong, C. W. *Appl. Phys. Lett.* **2007**, *91*, 161114.
(7) Hennessy, K.; Badolato, A.; Tamboli, A.; Petroff, P. M.; Hu, E.; Atature, M.; Dreiser, J.; Imamoglu, A. *Appl. Phys. Lett.* **2005**, *87*, 021108.
(8) Englund, D.; Faraon, A.; Fushman, I.; Stoltz, N.; Petroff, P.; Vuckovic, J. *Nature* **2007**, *450*, 857−861.
(9) Tanabe, T.; Nishiguchi, K.; Kuramochi, E.; Notomi, M. *Opt. Express* **2009**, *17*, 22505−22513.
(10) Mosor, S.; Hendrickson, J.; Richards, B. C.; Sweet, J.; Khitrova, G.; Gibbs, H. M.; Yoshie, T.; Scherer, A.; Shchekin, O. B.; Deppe, D. G. *Appl. Phys. Lett.* **2005**, *87*, 141105.
(11) Kolle, M.; Zheng, B.; Gibbons, N.; Baumberg, J. J.; Steiner, U. *Opt. Express* **2010**, *18*, 4356−4364.
(12) Pryce, I. M.; Aydin, K.; Kelaita, Y. A.; Briggs, R. M.; Atwater, H. A. *Nano Lett.* **2010**, *10*, 4222−4227.
(13) Frank, I. W.; Deotare, P. B.; McCutcheon, M. W.; Loncar, M. *Opt. Express* **2010**, *18*, 8705−8712.
(14) Perahia, R.; Cohen, J. D.; Meenehan, S.; Mayer Alegre, T. P.; Painter, O. *Appl. Phys. Lett.* **2010**, *97*, 191112.
(15) Scofield, A. C.; Shapiro, J. N.; Lin, A.; Williams, A. D.; Wong, P.-S.; Liang, B. L.; Huffaker, D. L. *Nano Lett.* **2011**, *11*, 2242−2246.
(16) Scofield, A. C.; Kim, S.-H.; Shapiro, J. N.; Lin, A.; Liang, B. L.; Scherer, A.; Huffaker, D. L. *Nano Lett.* **2011**, *11*, 5387−5390.
(17) Seo, K.; Wober, M.; Steinvurzel, P.; Schonbrun, E.; Dan, Y.; Ellenbogen, T.; Crozier, K. B. *Nano Lett.* **2011**, *11*, 1851−1856.
(18) Barclay, P. E.; Srinivasan, K.; Borselli, M.; Painter, O. *Electron. Lett.* **2003**, *39*, 842−844.
(19) McCutcheon, M. W.; Deotare, P. B.; Zhang, Y.; Loncar, M. *Appl. Phys. Lett.* **2011**, *98*, 111117.
(20) Choi, Y.-S.; Rakher, M. T.; Hennessy, K.; Strauf, S.; Badolato, A.; Petroff, P. M.; Bouwmeester, D.; Hu, E. L. *Appl. Phys. Lett.* **2007**, *91*, 031108.
(21) Riedrich-Moller, J.; Kipfstuhl, L.; Hepp, C.; Neu, E.; Pauly, C.; Mucklich, F.; Baur, A.; Wandt, M.; Wolff, S.; Fischer, M.; Gsell, S.; Schreck, M.; Becher, C. *Nat. Nanotechnol.* **2011**, *7*, 69−74.
(22) Lee, J. N.; Park, C.; Whitesides, G. M. *Anal. Chem.* **2003**, *75*, 6544−6554.
(23) Spaeth, K.; Kraus, G.; Gauglitz, G. *Fresenius J. Anal. Chem.* **1997**, *357*, 292−296.
(24) Xu, F.; Durham, J. W., III; Wiley, B. J.; Zhu, Y. *ACS Nano* **2011**, *5*, 1556−1563.
(25) Akogwu, O.; Kwabi, D.; Midturi, S.; Eleruja, M.; Babatope, B.; Soboyejo, W. O. *Mater. Sci. Eng., B* **2010**, *170*, 32.
(26) Manjavacas, A.; Garcia de Abajo, F. J. *Nano Lett.* **2009**, *9*, 1285−1289.
(27) Lipson, M. *IEEE J. Sel. Top. Quantum Electron.* **2006**, *12*, 1520−1526.
(28) Yao, J.; Liu, Z.; Liu, Y.; Wang, Y.; Sun, C.; Bartal, G.; Stacy, A. M.; Zhang, X. *Science* **2008**, *32*, 930.
(29) Babinec, T. M.; Hausmann, B. M.; Khan, M.; Zhang, Y.; Maze, J.; Hemmer, P. R.; Loncar, M. *Nat. Nanotechnol.* **2010**, *5*, 195−199.
(30) Englund, D.; Shields, B.; Rivoire, K.; Hatami, F.; Vuckovic, J.; Park, H.; Lukin, M. *Nano Lett.* **2010**, *10*, 3922−3926.